

THE THIRD EYE OF SOLDIERS: PORTABLE UAVS IN BATTLE FIELDS

Shuo Huang^a, Jian Lu^a, Lin Xie^b and Jindong Tan^a

^aDepartment of Electrical and Computer Engineering

^bDepartment of Mechanical Engineering Michigan
Technological University, Houghton, MI 49931 E-mail:
shuoh, jilu, linx, jitan@mtu.edu

Abstract

This paper presents a novel adaptive sampling method using intelligent UAVs in battlefields to help soldiers with awareness of environments. A UAV can perform as a robotic wingman in soldier formations, compensating for that cannot be scouted by soldiers even being exposed to enemy fire. With portable size, the UAV is easily carried and flown for scouting tasks anytime. The flexibility of UAVs makes it possible to collect measurements sequentially. Each measurement is adaptively designed and determined from the Bayesian perspective to increase the fidelity of battlefields. Wavelet structure is considered to optimize measurement projections to substantially reduce the number of measurements based on compressive sensing framework. More specifically, each measurement is optimized by maximizing the posterior variance inferred from existing informative data. A motion planning algorithm for UAVs is designed based on the distribution of optimal measurements, striking a balance between moving cost and measurement value. Simulation results and future experimental environments are presented at last.

I. INTRODUCTION

This paper is focusing on adaptive sampling based on UAVs in battlefields, which is established on the emerging research work of mobile adaptive sensing and down-sampling methods. To collect measurements from dynamic battlefields, both soldiers and unmanned vehicles can be involved. Soldiers can collect battlefield information in their surrounding areas. However, it is usually impossible and very dangerous to collect information from where enemy firepower can cover. By adopting UAVs, measurements can be collected in a more flexible way. UAVs are equipped with more advanced sensors and computational devices. As mobile robotic sensors, the mobility allows them to reconfigure themselves according to sensing requirements. With increasing research interest in mobile robotic sensors due to their wide applications [1]– [5], researchers are becoming more aware of the advantages of using mobile sensors to monitor and recover dynamic environments.

In practical applications, mobile sensors always collect measurements excessively, causing a waste of sensing resources. Typically, Singh *et. al.* [3] have proposed an adaptive sampling algorithm to sample and reconstruct a spatial map using mobile sensors, however, with a coarse survey before adaptive refinement, a portion of which may be regarded as excessive measurements containing less useful information. Furthermore, mobile robotic sensors are always constrained by limited energy, sensor capability, and other environmental factors, influencing their sensing capabilities. These suggest that only the most informative data should be collected to avoid wasting sensing resources especially in battlefields, where more casualty can be caused due to additional scout. Compared with sampling schemes that use invariant strategies involving a

uniform sampling scheme, it leaves open problems on how to evaluate, determine, and collect the most informative measurements.

In the real world, the most informative data always concentrates at some particular locations that can be inferred or predicted. Most natural signals are sparse or compressible under certain domains, which means some or even many components of signals can be discarded. Therefore, it will be a waste of time and sensing resources to collect measurements of these components. Partial measurements containing most informative data are enough to represent target sensing fields with acceptable errors. Compressive sensing [6] guarantees signals can be recovered from incomplete measurements with little information loss. Motivated by compressive sensing, the number of measurements can be substantially reduced with acceptable reconstruction errors. Traditional compressive sensing methods collect random measurements, which have been proved to be of efficiency and high-performance in the field of digital signal and image processing. However, the number of measurements can be further reduced to improve sampling efficiency, if the latent features of signal itself can be explored to locate the most informative data.

Researchers working on Bayesian compressive sensing have made efforts to further reduce the number of measurements. Duarte *et. al.* [7] have proved the number of compressive sensing measurements can be substantially reduced, considering target signal features from the Bayesian perspective. Based on the signal dependency under a sparse domain, each measurement can be individually designed and optimized. Given a set of incomplete measurements, the original signal distribution can be inferred. Thus, it is possible to determine new measurements that can maximize the posterior variance to

decrease the sensing field uncertainty. This suggests to follow up a loop to determine adaptive measurements sequentially that each measurement is the most informative given all existing ones.

This paper develops an adaptive approach to sample and recover battlefields by collecting a small number of measurements using UAVs. This approach features flexibility and adaptability. To monitor and recover dynamic environments, this method involves fast sampling, processing, and re-sampling scheme. The way to increase sampling efficiency is to collect a small number of measurements, but the most informative ones. It is also critical to efficiently allocate sensing resources between sampling and mobile sensor moving. Since mobile sensors are restricted by multiple factors, including energy constraints, sensor capabilities, etc, measurement collection is also subject to UAVs moving cost.

The sampling algorithm in this paper is built based on compressive sensing, collecting only the most informative data. Compressive sensing is considered in the Bayesian perspective. Wavelet structure and statistical properties of given signals will be observed from existing incomplete measurements. New measurements are determined by exploiting these latent features, and collected by mobile robotic sensors sequentially. Mobile sensors (UAVs) provide the flexibility to sequentially sample a target sensing field. Motion planning is proposed to strike the balance between the information amount of each measurement and moving cost from current sensing position to the next candidate one. The algorithm alternates between determining measurements and collecting measurements. Since each measurement is carefully designed and locally optimized to contain more information, the number of measurements is smaller than that of compressive sensing methods involving random measurements. In this paper, the statistical model of compressive sensing under wavelet tree structure is introduced as preliminary knowledge. Iterations to determine and collect the most informative measurements are elaborated. Existing research work is reviewed, and experimental results are shown at last.

II. PRELIMINARY KNOWLEDGE

This paper is based on compressive sensing. The basic compressive sensing idea involves down-sampling phase and signal reconstruction phase. This paper develops adaptive sampling scheme based on mobile platforms for the former one. This section briefly summarizes the preliminary research work about statistical compressive sensing and wavelet tree structure that will be used in presenting the proposed adaptive sampling approach.

A. Compressive Sensing Model

Compressive sensing reconstructs a target signal by using incomplete measurements. Given an unknown signal x with the dimension of $N \times 1$, it is required at least N measurements in traditional sampling methods. In compressive sensing, a measurement matrix Φ projects the signal from higher dimension (N) to lower dimension (M) with $M < N$, generating the measurement set y with M elements, subject

to $y = \Phi x$. Obviously, it cannot be solved directly, since there are more unknown variables than equations. Thus, in compressive sensing it requires the target signal x is either sparse or compressible (sparse under another domain) to reduce the number of unknown entries. A sparse signal of dimension $N \times 1$ with the sparsity K indicates that there are only K significant entries, and $N - K$ zero or very small entries. Usually, the K is far smaller than the N . To sparsely represent the target signal x , it is supposed that s is the sparse representation with $x = \Psi^T s$, where Ψ is a particular sparse basis. Ψ could be the I matrix if x is sparse already. Therefore, the basic compressive sensing equation is given

$$y = \Phi x = \Phi \Psi^T s \quad (1)$$

With a sparse s that has only K significant values ($K < M$), the system can be solved. Only K unknown variables have to be dealt with rather N ($K \ll N$), thus reducing the signal complexity.

The compressive sensing model in Equ. (1) is popularly used in many applications. Based on this basic compressive sensing model, statistical compressive sensing model has been studied. Signals in the CS system as shown in Equ. (1) are modeled under Gaussian distributions, so that statistical features can be used. In statistical models, the sparse representation s is decomposed as the sum of two items with significant values and small values separately, $s = s_m + s_e$, where s_m is established by replacing small entries with zeros, and s_e is established by setting significant entries zero. Both the significant and the small values can be modeled as Gaussian random variables with significant and small variances. However, the second item is always regarded as Gaussian noises. The system equation is given

$$y = \Phi \Psi^T s_m + \Phi \Psi^T s_e = \Phi \Psi^T s_m + n_e \quad (2)$$

where n_e , the insignificant item, is regarded as a sort of noise. In Equ. (2), the measurement noise is ignored. With the consideration of measurement noise, the system equation can be expressed as

$$y = \Phi \Psi^T s_m + n_e + n_w = \Phi \Psi^T s_m + n_0 \quad (3)$$

where n_w is the measurement noise, and n_0 is the total noise in the system. The total noise is modeled within Gaussian distributions, $n_0 \sim N(0, \alpha_0^{-1})$ with $\alpha_0^{-1} = \sigma_0^2$. Thus, the compressive sensing measurements y can be regarded as a multivariate Gaussian distribution

$$y \sim N(\Phi \Psi^T s_m, \alpha_0^{-1} I) \quad (4)$$

The Gaussian distributions illustrate statistical features of target signals. In this paper, a particular sparse domain, Haar wavelet is used, and the statistical features are used to exploit the hidden signal structure under Haar wavelet domain.

B. Wavelet Tree Structure

Compressive sensing considers signal reconstruction under sparse domains. Haar wavelet domain is a popular used sparse domain, under which signals appear different scales of repeated patterns besides the sparseness. Signals are quite

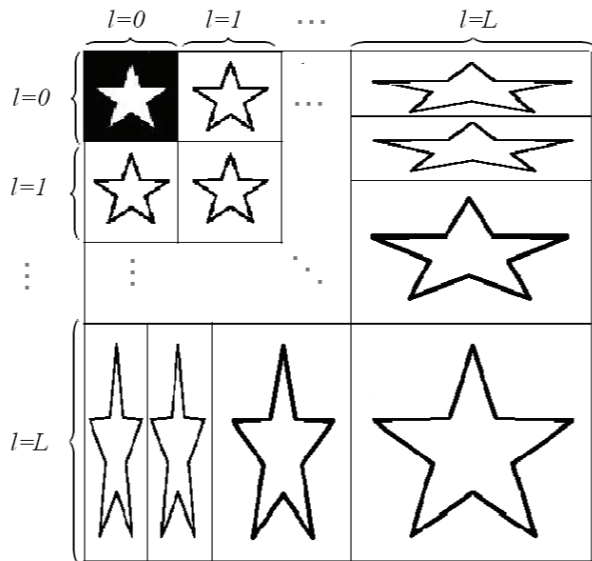


Fig. 1. Wavelet structure.

related between adjacent scales, forming the wavelet tree structure. Recent research has proved that the number of CS measurements can be further reduced by exploiting the wavelet tree structure. This structure can be observed under the Haar wavelet domain. In this paper, wavelet tree structure is studied to optimize adaptive measurements.

In traditional compressive sensing, random samples are always collected [6], and the signal is directly reconstructed without considering the dependencies of entries of the sparse representations. By exploiting the signal structure, Baraniuk *et al.* [8] prove that CS performance can be improved. The wavelet-tree structure [9] provides a powerful tool to explore signal structure under Haar Wavelet domain. In this paper, Ψ in Equ. (1) represents the Haar wavelet domain, and Fig. 1 illustrates the structure of the wavelet tree. In Fig. 1 the signal is repeated at different scales, $l = 0 \dots L$. Each coefficient in upper scale (smaller scale number) has four children coefficients in the adjacent lower scale. Whether the coefficient in lower scale is significant or insignificant depends quite a lot on whether its parent is significant or not. Thus, two states can be defined to illustrate the significant or insignificant value. Given a compressive sensing model in Equ. (1), the entries of the sparse representation s are modeled in two states, “high” and “low”, corresponding to the significant and small values separately. It is believed that one coefficient is likely to be significant, if it has a parent of significance, and *vice versa*. Therefore, in the sparse representation, no entry is independent. The dependency between entries is exactly the latent feature to be explored that will benefit measurement selection.

Each of the wavelet coefficients s is modeled as a Gaussian random variable

$$s_i \sim N(0, \sigma_i^2), i = 1 \dots N \quad (5)$$

where the variance σ_i^2 is written as α_i^{-1} in most literatures, indicating the precision of Gaussian distributions. To illustrate

the “likely to be significant or small” relationship, the variance is considered in two aspects, zero(or nearly zero) and non-zero(or significant), corresponding to “low” and “high”. The transition-probability matrix P at scale l is defined as $P(1,1) = 1 - \pi_l^0$, $P(1,2) = \pi_l^0$, $P(2,1) = 1 - \pi_l^1$, $P(2,2) = \pi_l^1$. The $P(i,j)$ indicates the probability of a child in state j given its parent in state i . Thus, the variance of each wavelet coefficient locates in a mixture distribution

$$\sigma_i^2 = (1 - \pi_i)\epsilon\tau_i^2 + \pi_i\tau_i \quad (6)$$

where ϵ is a very small value, and τ is the original variance. The small value ϵ could be zero, but does not has to be, since the precision is used $\alpha_i = \sigma_i^{-2}$. Each wavelet coefficient maintains two mixture parameters π_i except that in the root scale ($l = 0$), which indicates two possible different states of the corresponding parent.

$$\pi_i = \begin{cases} \pi_i^0 & \text{if } s_{pa(i)} = 0 \\ \pi_i^1 & \text{if } s_{pa(i)} \neq 0 \\ \pi_i^r & \text{if } \text{root scale} \end{cases} \quad (7)$$

$p_{pa(i)}$ is defined as the parent coefficient of coefficient s_i . For $S_{pa(i)} = 0$, it means $\sigma_i = \epsilon\tau_i$, corresponding to the first item in Equ. (6). For the coefficients at root scale, there is no parents existing, and they are considered as significant values all the time.

III. ADAPTIVE SAMPLING USING MOBILE SENSORS

Adaptive sampling is presented in details in this section. This adaptive sampling is based on compressive sensing. Compressive sensing collects random measurements without considering impact of each measurement. Adaptive sampling follows up an iterative procedure to generate measurements by mobile robotic sensors step by step to make sure each measurement is the most informative one given existing measurements. A mobile sensor requires some initial information before adaptively collecting measurements. In battlefields, informative data from soldiers are regarded as initial information for UAVs to adopt adaptive measurement collection. New measurements are collected to increase the fidelity and resolution given existing measurements.

Fig. 2 shows the adaptive sampling and reconstruction framework for a block. This framework includes six major parts, *initial measurements*, *mean and variance estimate*, *measurement determination*, *motion planning*, *parameter update*, and *signal reconstruction*. In *initial measurements*, a small portion of battlefields information is given at the very beginning. Then, compressive sensing model in Equ. (1) is established with Φ as the initial random measurement matrix. An iterative process is used to determine and collect measurements. New measurements will be inferred from posterior information of the current block given existing measurements from the Bayesian perspective. *mean and variance estimate* approximates the posterior mean and variance of the wavelet coefficients under Haar Wavelet domain. The π parameter introduced in II is used to estimate posterior mean and variance, and will be updated in the following process. Once the posterior mean and variance are obtained, *Measurement*

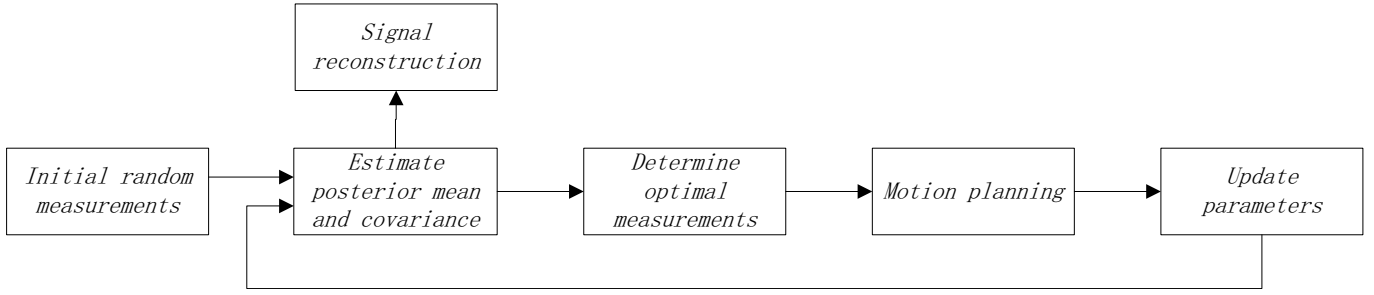


Fig. 2. Framework of adaptive sampling & reconstruction.

determination chooses optimal measurements to maximize the posterior variance. The measurement of the maximal posterior variance indicates to diminish the sensing field uncertainty to the most extent. However, for a mobile sensor the moving cost has to be considered. *Motion planning* makes a trade-off between measurement importance and sensor motion, and confirm the position of the next measurement from a few candidate positions. The new measurement is collected after the motion is confirmed and accomplished. *Parameter update* generates more accurate parameters given all the existing measurements. Accurate π would result accurate measurement inference. Each of the four-step iterations ends up with a new row ϕ_{new} added into the measurement matrix Φ and a new measurement set y_{new} generated. In the next iteration, all the computation is based on the newly generated Φ and y . The sampling iteration terminates, once enough measurements are collected. Signal is then reconstructed for current block, and mobile sensor will move to an adjacent block for more exploration.

A. Estimate Posterior Mean and Variance

For each block, a set of initial random measurements has to be collected as the basic information. Then new measurements are generated step by step. Each measurement is determined from existing information, more specifically the posterior variance of the target signal. In this part, posterior mean and variance estimation is shown.

In this paper, both y and s are regarded as Gaussian variables, which are determined by mean and variance. To approximate the signal, it is important to infer the mean and variance. In the compressive sensing system, the sparse representation s (wavelet coefficients) is subject to multivariate Gaussian distributions. Given a measurement set y , the posterior distribution of s is given in [10]

$$p(s|y, \alpha, \alpha_0) = \frac{p(y|s, \alpha_0)p(s|\alpha)}{p(y|\alpha, \alpha_0)} \quad (8)$$

where $\alpha = \{\alpha_1, \alpha_2, \dots, \alpha_N\}$, and α_i corresponds to the Gaussian precision of each Wavelet coefficient. $p(y|s, \alpha_0)$ and $p(s|\alpha)$ are Gaussian distributions from Equ. (4) and Equ. (5). $p(y|\alpha, \alpha_0)$ is a likelihood function for α and α_0 , being given

$$\begin{aligned} \mathcal{L}(\alpha, \alpha_0) &= p(y|\alpha, \alpha_0) = \int p(y|s, \alpha_0)p(s|\alpha)ds \\ &= (2\pi)^{-\frac{N}{2}} \left| \frac{I}{\alpha_0} + \Phi A^{-1} \Phi^T \right| \exp\left\{ \frac{I}{\alpha_0} + \Phi A^{-1} \Phi^T \right\} \end{aligned} \quad (9)$$

Since the three distributions in Equ. (8) are known, the posterior distribution of s can be calculated. Given a set of measurements y , it can be calculated that $s|y, \alpha, \alpha_0 \sim N(\mu, \Sigma)$ with posterior mean and variance, yielding

$$\mu = \alpha_0 \Sigma \Phi^T y \quad (10)$$

$$\Sigma = (\alpha_0 (\Phi \Psi^T)^T \Phi \Psi + A)^{-1} \quad (11)$$

where $A = \text{diag}(\alpha_1, \alpha_2, \dots, \alpha_N)$.

With the posterior mean and variance calculated, it is worth noting that the parameters in Equ. (9), which is a likelihood function, can be optimized in order to infer new precisions given the posterior mean and variance. To optimize parameters in Equ. (9) is to maximize $\mathcal{L}(\alpha, \alpha_0)$, so that the best α and α_0 can be found for the distribution. This is known as the type-II maximum likelihood, and can be implemented through differentiation, being given in [10]. The new parameters yield:

$$\alpha_i^{new} = \frac{\gamma_i}{\mu_i^2} \quad (12)$$

$$1/\alpha_0^{new} = \frac{\|y - \Phi \mu\|_2^2}{N - \sum \gamma_i} = \frac{\|y - \Phi \mu\|_2^2}{\sum \pi_i} \quad (13)$$

where $\gamma_i = 1 - \alpha_i \Sigma_i i$.

An iterative algorithm can be executed by alternating between Equ. (10) (11) and Equ. (12) (13). The convergence is very fast, and α_i becomes large for zero or small wavelet coefficients.

In Haar Wavelet domain, signals have special associations between adjacent scales, suggesting that the parameter α can be further optimized. From Equ. (6), it can be seen that the wavelet structure can be imposed to the variance. Thus, the same structure can be imposed to Equ. (12), resulting

$$1/\alpha_i^{new} = (1 - \pi_i) \epsilon \frac{\mu_i^2}{\gamma_i} + \pi_i \frac{\mu_i^2}{\gamma_i} \quad (14)$$

The iterative algorithm has been changed to alternating between Equ. (10) (11) and Equ. (14) (13). The posterior mean and variance can be approximated with a few iterations.

B. Measurement Determination

With the estimation of posterior mean and covariance, new measurements are to be determined to achieve local optimum. The basic idea to determine a new measurement is to add a new row to the measurement matrix Φ , such that the resulting measurement would have the maximal posterior variance. The maximal posterior variance indicates the most uncertainty, and

a measurement with maximal posterior variance is to diminish the uncertainty to the most. Suppose as a time instant, k measurements have been collected with the given measurement matrix $\Phi = [\phi_1^T, \phi_2^T \cdots \phi_k^T]^T$. The aim in this step is to determine a new row ϕ_{k+1} and add it into the measurement matrix Φ .

After a few iterations addressed in Section III-A, the latest covariance is computed given new α and α_0

$$\Sigma^{new} = (\alpha_0^{new} (\Phi \Psi^T)^T \Phi \Psi + A^{new})^{(-1)} \quad (15)$$

where $A^{new} = \text{diag}(\alpha_1^{new}, \alpha_2^{new} \dots \alpha_N^{new})$.

In [11], new measurements are determined by maximizing the posterior covariance under sparse domain. In this section, new measurement will be determined in the spatial domain by maximizing the posterior variance of new measurement

$$\text{Var}(y_{k+1}) = \phi_{k+1} \Psi^T \Sigma^{new} (\phi_{k+1} \Psi^T)^T \quad (16)$$

The larger the variance is, the more uncertain the measurement is, indicating this particular measurement contains more valuable information. The parameter is found by maximizing this quantity

$$\hat{\phi}_{k+1} = \arg \max_{\phi_{k+1}} \text{Var}(y_{k+1}) \quad (17)$$

which is the locally optimized measurement. There might be millions of new row forms. It is impossible to go through all of them and determine an optimal one. The candidate new measurements are chosen from a pre-designed library of a small number of elements, subject to the particular sensing pattern of mobile robotic sensors used.

C. Motion Planning

The optimal measurement determined above is the most informative one without considering any motion planning. With mobile sensor involved, motion planning is also an important part. Measurements have to be determined not only subject to the maximal posterior variance but also the moving cost from current position to the newly determined measurement position.

Based on the description in Section III-B, one measurement is determined as the local optimum. However, it would be wasteful if the mobile sensor go back and forth to collect measurements. To plan the motion of mobile sensors, the moving cost should be considered. Not the most informative measurement is collected, but the one which strikes the balance between information content and moving cost. Thus, Equ. (17) should be changed by adding a moving cost item.

$$\hat{\phi}_{k+1} = \arg \max_{\phi_{k+1}} (\text{Var}(y_{k+1}) - \omega C(\phi_k, \phi_{k+1})) \quad (18)$$

where the first item remains the same as Equ. (17), and the second item represents the moving cost. $C(\cdot, \cdot)$ is a function indicating the moving cost between the two measurement positions, and $C(\phi_k, \phi_{k+1, i})$ represents the moving cost from current sensing position to the next one. ω is a weighted factor that is used to achieve a proper ratio for these two items. In plane area, the moving cost is usually proportional to the moving distance. However, in the real applications, many other

factors have to be considered, including mobile sensor turning, obstacles, collisions, etc. In this paper, we fairly assume the moving cost is proportional to the moving distance.

The situation in Equ. (18) can be further simplified. A few candidate measurements can be generated using Equ. (17), which should be the most informative ones. It is supposed that n candidate measurements are generated, denoting as $\phi_{k+1,1} \cdots \phi_{k+1,n}$. The new measurement is chosen simply by

$$\hat{\phi}_{k+1} = \arg \min_{\phi_{k+1, i}} C(\phi_k, \phi_{k+1, i}) \quad i = 1 \cdots n \quad (19)$$

In ideal situations, it is exactly the closest one to the current sensing position. From the experimental results, these two strategies do not differ much. Thus, the latter one is chosen, since the calculation can be simplified, and precessing time can be saved.

The paragraphs above have addressed how to determine one new measurements. However, in real experiments, this is a process requiring a lot of computation. To reduce computation load as well as save time, the strategy goes in two steps alternating between generating a few new measurements as addressed above and collecting all of them. When n candidate measurements are generated, the problem is converted to a travelling salesman problem (TSP). It is to collect all these measurements with the minimal moving cost. Before all the n measurements are collected, no new candidate measurements will be generated. Once finished, another n candidate measurement are generated. TSP belongs to the class of NP-complete problems. In this part, we just choose the candidate measurement with minimal moving cost as the next one. As measurements are collected, the number n would finally reduce to 1. Then, a new round can be performed generating a few more candidate measurements, and collecting one by one.

D. Parameter Update

The aim to update π is to approximate the distribution of s more accurately, including π_i for each wavelet coefficient. The concept of conjugate prior is used, which can estimate variables more accurately with known samples. *Beta* distribution is the conjugate prior of a binomial distribution given some existing samples.

The paradigm shown in Fig. 2 contains for major parts for each loop. The parameter π_i indicates whether the wavelet coefficient is significant or not, while the latest α generated in *estimate posterior mean and variance* and used in Equ. (15) for each loop has the same meaning. Thus, the update of parameter π_i uses all the α_i generated in prior loops. Supposing at the k th loop, there are $k-1$ α_i that can be used to to estimation π_i , denoting as $\alpha_i^{new(j)}$, $j = 1 \dots k-1$.

The π parameters are updated by

$$p(\pi_i^0 | -) = B \left(e_0^{i0} + \sum_j 1(\alpha_i^{new(j)} \ll \text{Inf}, \alpha_{pa(i)}^{new(j)} = \text{Inf}), \right. \\ \left. f_0^{i0} + \sum_j 1(\alpha_i^{new(j)} = \text{Inf}, \alpha_{pa(i)}^{new(j)} = \text{Inf}) \right) \quad (20)$$

$$p(\pi_i^1 | -) = B \left(e_0^{i1} + \sum_j 1(\alpha_i^{new(j)} \ll \text{Inf}, \alpha_{pa(i)}^{new(j)} \ll \text{Inf}), \right. \\ \left. f_0^{i1} + \sum_j 1(\alpha_i^{new(j)} \ll \text{Inf}, \alpha_{pa(i)}^{new(j)} = \text{Inf}) \right) \quad (21)$$

$$p(\pi_i^r | -) = B \left(e_0^{ir} + \sum_j 1(\alpha_i^{new(j)} \ll \text{Inf}), \right. \\ \left. f_0^{ir} + \sum_j 1(\alpha_i^{new(j)} = \text{Inf}) \right) \quad (22)$$

where $1(x)$ denotes an indicator function. $1(x) = 1$ for true statement x , and 0 otherwise.

Iterations containing the above four steps carry on until enough measurements are collected. Signals are reconstructed given both initial random measurements and adaptive measurements. To reconstruct signal, probabilistic methods are used. More details about reconstruction is shown in next section.

IV. SIMULATIONS AND EXPERIMENTS

In this section, possible experimental environment is introduced and two simulations are presented using the sampling method addressed in this paper. To reconstruct the signal, the MCMC method addressed in [12] is applied.

A. Experimental Environments in Battlefields

The awareness of environments is important for any soldier in battlefields. However, in real situations, soldiers are unable to observe all the perspectives due to the complex environments and enemy fire power. Scout, battlefields surveillance, target acquisition, etc, are always dangerous tasks that may cause unexpected casualties. An intelligent portable UAV equipped with vision sensors can provide extra information that cannot be observed from soldiers' perspectives. With the help of the UAV, soldiers become more aware of battlefields situation, and make correct decisions to reduce casualties.

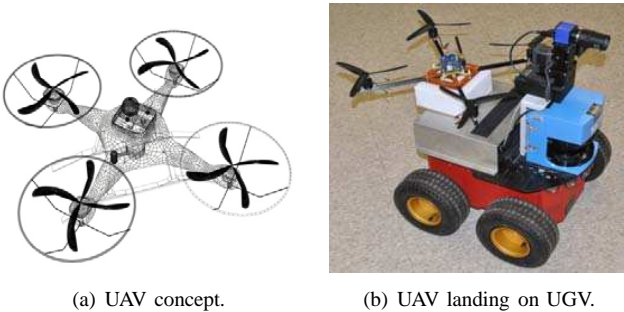


Fig. 3. Portable UAV.

Fig. 3(a) shows the concept of the portable UAV. It is of small size, foldable and easily carried. Soldiers carrying the UAV can fly it anytime for overlook scout. Thus, the UAV

can start scouting anywhere soldiers can reach, and reach where soldiers cannot reach. The UAV is equipped with vision sensors, including cameras and infrared to acquire valuable battlefields information. To enhance the on ground moving ability, a UGV is used as a landing station for the UAV as shown in Fig. 3(b). It can move conveniently and hide in grass. It is also equipped with powerful sensors, including camera, laser scanner, ultrasonic, etc, and can be assigned with some scouting tasks. Both the UAV and the UGV can be special members in soldier formations. In Fig. 4, the formation includes the mixture of the UAV, UGV, and soldiers. Soldiers can communicate with each other, as well as the UAV and UGV. The unmanned vehicles and soldiers build up a powerful vision system to monitor uncertain factors in the battle field avoiding unnecessary sacrifice. The overall system is well networked, in which wireless links between them guarantee real-time data exchange. Soldiers acquire valuable battlefields information from UAV, while the UAV accomplish tasks according to both commands and informative data from soldiers.

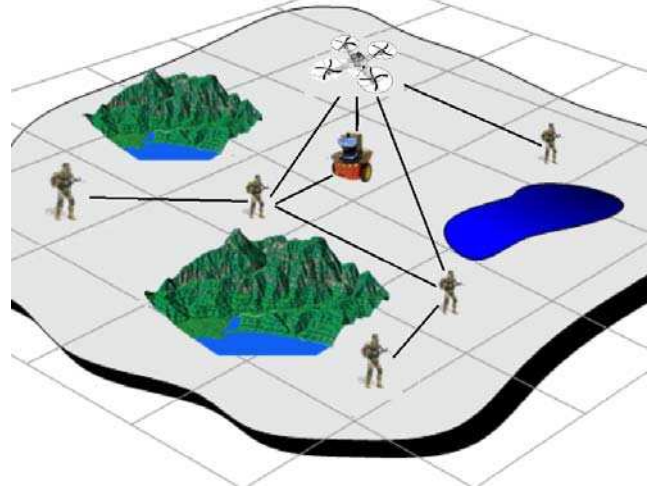


Fig. 4. Networked Battlefields system.

In the battlefields, omniview is crucial for soldiers to make tactic decisions and execute scout and surveillance tasks, avoiding unnecessary casualties. However, neither soldiers nor unmanned vehicles can generate omniview of the overall environment from their own vision sensors. Thus, information collected from each unit of soldiers and unmanned vehicles in the networked vision system is fused together. The fused information can be used to guide tactical movement of both unmanned vehicles and soldiers. Data is transmitted through high-speed wireless links between them. To generate a better and faster omniview, multi UAVs can be used to collect data simultaneously. Multi UAVs can collaborate to find proper sensing positions and deploy themselves for valuable information acquisition.

In the dynamic networked system formed by unmanned vehicles and soldiers in battlefields, self-navigation is required for UAVs, especially when they fly temporarily out of the communication range of soldiers or it is unclear from soldiers' views. It can adaptively collect the most important measure-

ments to increase battlefields fidelity and execute surveillance or scout tasks autonomously. There are two ways for self-navigation. The first is to recognize target by equipped sensors, including cameras, lasers, etc. Sensors can acquire and filter target information in battlefields, which should be paid more attention. Once targets are located, UAVs can collect more information regarding the target. The other way occurs, when no obvious targets can be found, which is also the main focus of this paper. In this case, a Bayesian analysis process is executed as addressed in Section III to determine new measurements. Existing data will be analyzed and posterior distributions of battlefields signals will be inferred. Soldiers can send commands to interrupt any ongoing tasks based on self-navigation via real-time communication, since soldiers' commands have the highest priority. Feedback can also be read from unmanned vehicles for soldiers to change tactic deployment accordingly.

B. Simulation Results

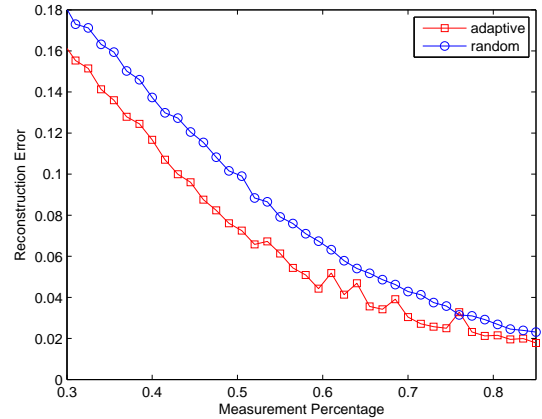
Due to the experimental conditions, only simulations are performed to justify the efficiency of the adaptive sampling method presented in this paper. In the following simulations, mobile sensors are used to adaptively collect informative data. A small portion of initial random measurements are used to simulate soldiers' observations in real battlefields. In this section, two simulations are done. In the first simulation, average reconstruction performance is evaluated by comparing reconstructed signals with original signals. The errors between them indicate the reconstruction performance. In the second one, a particular simulation is given, Great Lakes ice cover reconstruction. In the latter one, the experiment is compared with another adaptive sampling method. All the computations in this section were performed using Matlab run on a server with two Intel Xeon 5130 CPUs working at 2G and 8G DDR2 memory.

1) *Average Performance*: To evaluate the average performance, we reconstruct an image in Fig. 5(b). Measurements are collected in both adaptive way and random way. The experiments are repeated many times for the average performance. All measurements are collected in the spatial domain and assumed 0 measurement noise. Suppose the original image in Fig. 5(b) is x , each measurement can be represented as $y_i = \phi_i x = \phi_i \Psi^T s$, where s should be the 2-D wavelet transform of the original image. We assume a mobile sensor can only cover a small area in the image, A_{small} which is supposed to be m by m . Thus, each measurement y_i is a linear combination of all elements in the corresponding small area defined, and in each row of the measurement matrix ϕ_i , there exists only m by m non-zero entries. The coefficients of the combination are drawn from a standard Gaussian distribution with 0 mean and 1 variance. To evaluate the reconstruction performance, reconstruction error is introduced as $\|x_{rec} - x\|_2 / \|x\|_2$, where x and x_{rec} represent original and reconstructed signals separately.

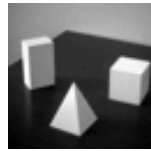
We consider the reconstruction of a 32 by 32 image. The original image and reconstructions of different ratios of adaptive measurements are shown in Fig. 5. To reconstruct

the image, each measurement collected is restricted within a 5×5 area with weighted factors drawn from $N(0, 1)$. 15 best candidate measurements are determined each time, and the closest one is chosen as the position where mobile sensor has to visit to collect measurements. Original image we used to reconstruct is shown in Fig. 5(b). Supposing to reconstruct Fig. 5(b) we have a set of random measurements in advance. A mobile sensor would collect some optimal measurements. The red line indicates the reconstruction error of the random measurements, where the total percentage is shown in the figure. The blue line in Fig. 5(a) is generated by choosing 250 (about 25%) random measurements at the very beginning, and adaptive measurements as the rest. Each point on the curves is generated by averaging 50 reconstructions.

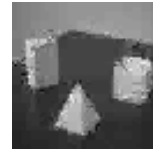
Fig. 5(c) shows the reconstruction result of 200 adaptive measurements collected one by one and 250 random measurements as a basic portion. Fig. 5(d) shows the reconstruction result of 450 random measurements. The reconstruction errors are 0.104 and 0.127 separately. As discussed in III, reconstructions with adaptive measurements outperform, and the reconstruction can be obviously improved when measurement percentage is relatively small. As measurement percentage increases, the error becomes very tiny, and the impact of adaptive measurements is not that significant.



(a) Reconstruction error.



(b) Original image.



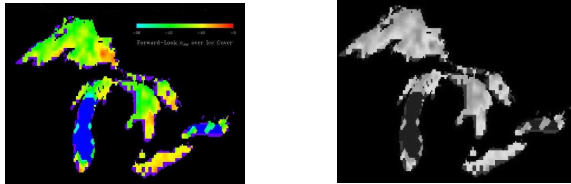
(c) Reconstruction with error 0.104.



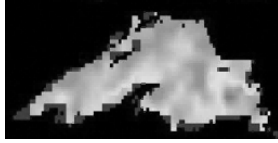
(d) Reconstruction with error 0.127.

Fig. 5. Reconstruction error comparison.

2) *Sampling & Reconstruction of Great Lakes Ice Cover*: In the second experiment, a potential application is discussed, that is, to sample and reconstruct the ice cover of Great Lakes. The ice cover of Great Lakes has great impacts on many aspects of life, including fishing industry, commercial shipping, potential flooding, etc. As an important indicator of regional climatic conditions, research work on ice cover of the world's largest freshwater surface has been paid a huge



(a) Ice cover RGB image. (b) Reconstruction gray scale image.



(c) Lake Superior ice cover.

Fig. 6. Great Lakes ice cover reconstruction.

amount of effort.

In this part of simulation, we fairly assume to monitor the Great Lakes ice cover using a mobile robotic sensor (UAV). Restricted by our experimental equipments, we only did simulations based an NOAA image. Fig. 6(a) shows the ice cover scenario of Great Lakes from NOAA web site ¹. In this simulation, it is supposed that a UAV can fly over the Great Lakes area and reconstruct the ice cover. To simplify the situation, the ice cover image in gray scale is used. The overall image is in the size of 576 by 448. 20% random measurements are initially generated, and 20% more adaptive measurements sequentially determined and collected given existing measurements. Once enough measurements are collected, a reconstruction algorithm is run to recover the ice cover image. Fig. 6(b) shows the reconstructed ice cover based on the algorithm addressed in this paper. In this gray scale figure, the pixel value ranges from 0 to 255. The reconstruction error is 0.2204 under the assumption that there is no measurement noise, which is computed as addressed in IV-B1.

At last of this simulation, our adaptive sampling method is compared with the two step adaptive sampling method addressed in [3]. In this part, we suppose to reconstruct the ice cover of Lake Superior as shown in Fig. 6(c). In this scenario, gray scale image with the size of 128 by 256 is generated, whose pixel value ranges from 0 to 255. Gaussian noise is added into the measuring process to approximate real measuring situations. Each measurement is added $5 \times N(0, 1)$ noise for both methods. To implement adaptive sampling method in [3], 50% measurements are collected in total, with 25% for the coarse survey and 25% for the refinement. For the adaptive sampling method in this paper, the same amount of total measurements are collected, that is, 25% random measurements and 25% adaptive measurements. After reconstruction, the method addressed in this paper performs a little better with the reconstruction error 0.2758, while the other one has error of 0.3541. In the experiment, the trajectory

of mobile sensor is also generated. Since the adaptive sampling method is considered in the Wavelet domain, the trajectory of mobile sensor is not that related with the actual image shape in Fig. 6(a). Thus, it is not shown in this paper.

V. RELATED WORK

The focus of this paper is to exploit a powerful data-adaptive sensing platform based on mobile robotic sensors. Adaptive sampling provides the opportunity to effectively allocate sensing resources. Adaptive sampling has been applied in many fields. Nowak *et al.* [13], propose a multi-step adaptive sampling, also named distilled sensing, which is shown to be an effective approach when detecting and recovering high-dimensional sparse signals with noise. Data-adaptive path planning schemes are investigated for both single mobile sensor and wireless networks of mobile sensor platforms [1], [3], resulting in reducing an impractically large number of pre-computed sensing elements to an affordable quantity. Moreover, the rich literature in adaptive sampling based on multi-robot platforms provides a large class of methods for wide-area exploration, mapping, and environmental monitoring. Zhang and Sukhatme [4] proposed an adaptive sampling algorithm for a mobile sensing network to estimate a scalar field subject to the constraint that mobile robots have limited energy.

Compressive sensing is an effective way to significantly reduce samples required to reconstruct sensing fields of interest. It is an emerging research field based on that a small number of linear measurements can recover a sparse or compressible signal without loss of any useful information [6], [14]–[16]. An orthogonal basis is always chosen to sparsely represent the original signals. By applying compressive sensing, the signal can be recovered from incomplete measurements generated by a sampling rate much lower than the requirements in Shannon sampling theory. Thus, it reduces the load at sampling stage. Random chosen linear measurements have been proven good reconstruction [16], [17]. The random linear measurements can be applied to many transform-based orthogonal bases, such as Fourier, wavelet, discrete cosinusoid [18]. Compressive sensing can be applied to many practical applications. Candes *et al.* [19] shows that image can be perfectly reconstructed by samples along radial lines rather than random projections. A promising new paradigm for networked data analysis is described in [20] to reconstruct sparse or compressible networked data in multi-hop networks and wireless sensor networks. Compressive sensing is also used in a mobile cooperative network [21] that is tasked with building a map of the spatial variations of interest with a small number of measurements. Baraniuk *et al.* develops a new camera architecture with only a single detection element [22].

Recent research on compressive sensing explores sparsity structure of target signals from the Bayesian perspective. With Bayesian approaches applied into the measuring phase of compressive sensing, a so-called adaptive compressive sensing is developed, where the measurement matrix is generated gradually, so that each measurement is particularly designed to maximize the information content to achieve local optimum.

¹<http://coastwatch.glerl.noaa.gov/overview/cw-overview.html#FIG1.5>

The desired signal has statistical characteristics which can be used to significantly reduce the number of compressive sensing measurements by the Bayesian inference [7], [8]. With compressive sensing signals modeled as Gaussian random variables, Tipping [10] gives the solution optimizing the variable parameters. Posterior mean and covariance are estimated through expectation-maximization algorithm. Based on posterior mean and covariance, Ji *et. al.* [23] propose a Bayesian compressive sensing framework which optimizes the measurement matrix by providing posterior belief of the sparse representation from the Bayesian perspective. Meng *et. al.* [24] applies Bayesian compressive sensing into wireless sensor networks for sparse event detection to reduce the number of wake-up sensors.

By applying Bayesian approaches into the decoding phase, recovery algorithms are enhanced. Signal models and measurement models are considered during recovery, resulting in less reconstruction noise, and faster computation. MCMC methods are used to infer new projections by drawing samples. He and Carin [12] demonstrate that substantially fewer projection measurements are sufficient to achieve accurate compressive sensing reconstruction via MCMC methods by analyzing the Wavelet tree structure of a signal. Similarly, Tan and Li [25] show that a sparse Bayesian learning algorithm and a block Gibbs sampling algorithm can be used to estimate the transform coefficient vector (sparse representation). Baron *et al.* [26] performs approximate Bayesian inference using belief propagation decoding to represent the measurement matrix as a graphical model based on available statistical characterization of the signal. Babacan *et. al.* [27] develop a greedy algorithm for fast reconstruction using Laplace priors to model the sparsity of the unknown signal.

VI. CONCLUSIONS AND FUTURE WORKS

In this paper, an adaptive approach is proposed to sample and reconstruct a given sensing field. This research work is based on the statistical model for Bayesian compressive sensing. The structure in wavelet coefficients of signals is exploited in the sampling process. It has been justified better performance in the simulation. Compared with compressive sensing involved random measurements and other adaptive method, smaller reconstruction error can be achieved by adaptively collecting measurements under the situation that the same amount of measurements and the same reconstruction methods are used. The proposed method has demonstrated modest motion cost when collecting adaptive measurements by mobile robotic sensors.

Real experiments will be carried out in the future. Experimental environment using multiple P3-AT robots and the UAV shown in Fig. 3(a) is to set up. Additionally, multi unmanned vehicle collaboration will be researched. Reconstruction performance will be compared with other reconstruction methods.

REFERENCES

[1] N. Yilmaz, C. Evangelinos, P. Lermusiaux, and N. Patrikalakis, "Path planning of autonomous underwater vehicles for adaptive sampling using mixed integer linear programming," in *IEEE Journal of Oceanic Engineering*, vol. 33, pp. 522–537, 2008.

[2] J. Leonard and H. Durrant-Whyte, "Mobile robot localization by tracking geometric beacons," *IEEE Transactions on Robotics and Automation*, vol. 7, no. 3, pp. 376–382, 1991.

[3] A. Singh, R. Nowak, and P. Ramanathan, "Active learning for adaptive mobile sensing networks," in *Proceedings of 5th International Conference on Information Processing in Sensor Networks*, pp. 60–68, 2006.

[4] B. Zhang and G. S. Sukhatme, "Adaptive sampling for estimating a scalar field using a robotic boat and a sensor network," in *IEEE International Conference on Robotics and Automation*, pp. 3673–3680, 2007.

[5] D. Popa, A. Sanderson, R. Komerska, S. Mupparapu, D. Blidberg, and S. Chappel, "Adaptive sampling algorithms for multiple autonomous underwater vehicles," in *IEEE/OES Autonomous Underwater Vehicles*, pp. 108–118, 2004.

[6] R. Baraniuk, "Compressive sensing [lecture notes]," in *IEEE Signal Processing Magazine*, vol. 24, pp. 118–121, 2007.

[7] T. Blumensath and M. E. Davies, "Sampling theorems for signals from the union of linear subspaces," in *IEEE Transactions on Information Theory*, vol. 55, pp. 1872–1882, 2009.

[8] M. F. Duarte, V. Cevher, and R. G. Baraniuk, "Model-based compressive sensing for signal ensembles," in *proceedings of 47th Annual Allerton Conference on Communication, Control, and Computing*, pp. 244–250, 2009.

[9] M. Crouse, R. Nowak, and R. Baraniuk, "Wavelet-based statistical signal processing using hidden markov models," in *IEEE Transactions on Signal Processing*, vol. 6, pp. 886–902, 1998.

[10] M. Tipping, "Sparse bayesian learning and the relevance vector machine," in *Journal of Machine Learning Research*, vol. 1, pp. 211–244, 2001.

[11] S. Ji and L. Carin, "Bayesian compressive sensing and projection optimization," in *Proceedings of the 24th international conference on Machine learning*, pp. 377–384, 2007.

[12] L. He and L. Carin, "Exploiting structure in wavelet-based bayesian compressive sensing," in *IEEE Transactions on Signal Processing*, vol. 57, pp. 3488–3497, 2008.

[13] J. Haupt, R. Castro, and R. Nowak, "Distilled sensing: selective sampling for sparse signal recovery," in *Proceedings of The 12th International Conference on Artificial Intelligence and Statistics*, pp. 216–223, 2009.

[14] E. Candes and M. Wakin, "An introduction to compressive sampling," in *Signal Processing Magazine, IEEE*, vol. 25, pp. 21–30, 2008.

[15] D. Donoho, M. Elad, and V. Temlyakov, "Stable recovery of sparse overcomplete representations in the presence of noise," in *IEEE Transactions on Information Theory*, vol. 52, pp. 6–18, 2006.

[16] E. Candes, J. Romberg, and T. Tao, "Robust uncertainty principles: exact signal reconstruction from highly incomplete frequency information," in *IEEE Transactions on Information Theory*, vol. 52, pp. 489–509, 2006.

[17] D. Donoho, "Compressed sensing," in *IEEE Transactions on Information Theory*, vol. 52, pp. 1289–1306, 2006.

[18] R. Baraniuk and P. Steeghs, "Compressive radar imaging," in *Radar Conference, IEEE*, pp. 128–133, 2007.

[19] E. Candes, J. Romberg, and T. Tao, "Robust uncertainty principles: exact signal reconstruction from highly incomplete frequency information," in *IEEE Transactions on Information Theory*, vol. 52, pp. 489–509, 2006.

[20] J. Haupt, W. Bajwa, M. Rabbat, and R. Nowak, "Compressed sensing for networked data," in *Signal Processing Magazine, IEEE*, vol. 25, pp. 92–101, 2008.

[21] Y. Mostofi and P. Sen, "Compressive cooperative sensing and mapping in mobile networks," in *American Control Conference*, pp. 3397–3404, 2009.

[22] M. Wakin, J. Laska, M. Duarte, D. Baron, S. Sarvotham, D. Takhar, K. Kelly, and R. Baraniuk, "An architecture for compressive imaging," in *IEEE International Conference on Image Processing*, pp. 1273–1276, 2006.

[23] S. Ji, Y. Xue, and L. Carin, "Bayesian compressive sensing," in *IEEE Transactions on Signal Processing*, vol. 56, 2008.

[24] J. Meng, H. Li, and Z. Han, "Sparse event detection in wireless sensor networks using compressive sensing," in *43rd Annual Conference on Information Sciences and Systems*, pp. 181–185, march 2009.

[25] X. Tan and J. Li, "Compressed sensing via sparse bayesian learning and gibbs sampling," in *IEEE 13th Digital Signal Processing Workshop and 5th Signal Processing Education Workshop*, pp. 690–695, 2009.

[26] D. Baron, S. Sarvotham, and R. G. Baraniuk, "Bayesian compressive sensing via belief propagation," in *IEEE Transactions on Signal Processing*, vol. 58, pp. 269–280, 2010.

[27] S. Babacan, R. Molina, and A. Katsaggelos, "Bayesian compressive sensing using laplace priors," in *IEEE Transactions on Image Processing*, vol. 19, pp. 53–63, 2010.